
Title	Computing plasma focus pinch current from total current measurement
Author(s)	S. Lee, S. H. Saw, P. C. K. Lee, R. S. Rawat and H. Schmidt
Source	<i>Applied Physics Letters</i> , 92(11): 111501. doi: 10.1063/1.2899632
Published by	American Institute of Physics

© 2008 American Institute of Physics. This article may be downloaded for personal use only. Any other use requires prior permission of the authors and the American Institute of Physics.

The following article appeared in Lee, S., Saw, S. H., Lee, P. C. K., Rawat, R. S., & Schmidt, H. (2008). Computing plasma focus pinch current from total current measurement. *Applied Physics Letters*, 92(11), 111501. doi:10.1063/1.2899632 and may be found at <http://dx.doi.org/10.1063/1.2899632>

Computing plasma focus pinch current from total current measurement

S. Lee,^{1,2,3,a)} S. H. Saw,² P. C. K. Lee,³ R. S. Rawat,³ and H. Schmidt⁴

¹*Institute for Plasma Focus Studies, 32 Oakpark Dr, Chadstone, Victoria 3148, Australia*

²*INTI International University College, 71800 Nilai, Malaysia*

³*Nanyang Technological University, National Institute of Education, Singapore 637616, Singapore*

⁴*International Centre for Dense Magnetized Plasmas, 00-908 Warsaw, Poland*

(Received 12 February 2008; accepted 25 February 2008; published online 18 March 2008)

The total current I_{total} waveform in a plasma focus discharge is the most commonly measured quantity, contrasting with the difficult measurement of I_{pinch} . However, yield laws should be scaled to focus pinch current I_{pinch} rather than the peak I_{total} . This paper describes how I_{pinch} may be computed from the I_{total} trace by fitting a computed current trace to the measured current trace using the Lee model. The method is applied to an experiment in which both the I_{total} trace and the plasma sheath current trace were measured. The result shows good agreement between the values of computed and measured I_{pinch} . © 2008 American Institute of Physics. [DOI: 10.1063/1.2899632]

The total current I_{total} waveform in a plasma focus discharge is easily measured using a Rogowski coil. The peak value I_{peak} of this trace is commonly taken as a measure of the drive efficacy and is often used to scale the yield performance of the plasma focus.^{1,2} This is despite the fact that yields^{3–5} should more consistently be scaled to focus pinch current I_{pinch} , since it is I_{pinch} which directly powers the emission processes. The reason many researchers use I_{peak} instead of I_{pinch} for scaling is simply that while I_{peak} is easily measured, I_{pinch} , which is the value of the plasma sheath current I_p at time of pinch, is very difficult to measure even in large devices where it is possible to place magnetic probes near the pinch.^{3–5} This measurement is also inaccurate and perturbs the pinch. In a small device, there is no space for such a measurement. A simpler method was tried to compute the I_p waveform using measured waveforms of I_{total} and tube voltage.^{6,7} This was achieved only up to the start of the radial phase thereby missing the crucial I_{pinch} . To date, I_{pinch} is still one of the least measured and often misunderstood quantities. In this connection, an attempt was made⁸ to compute the time of pinch. However, in that work, I_{pinch} was assumed to be I_{total} at pinch time.

The relationship between I_{pinch} and I_{peak} is not simple and has only been recently elaborated.⁹ It primarily depends on the value of the static inductance L_0 compared to the dynamic inductances of the plasma focus. As L_0 is reduced, the ratio $I_{\text{pinch}}/I_{\text{peak}}$ drops. Thus, yield laws scaled to I_{peak} will not consistently apply when comparing two devices with all parameters equal but differing significantly in L_0 . Better consistency is achieved when yield laws are scaled to I_{pinch} .

In this paper, we propose a numerical method to consistently deduce I_{pinch} from any measured trace of I_{total} . This method will improve the formulation and interpretation of focus scaling laws. Specifically, we define I_{pinch} as the value of I_p at the start of the quiescent (or pinch) phase of the plasma focus radial dynamics. We now discuss the distinction between I_{total} and the plasma sheath current I_p .

A measured trace of I_{total} is commonly obtained with a Rogowski coil wrapped around the plasma focus flange¹⁰ through which is fed I_{total} discharged from the capacitor bank between the coaxial electrodes across the back wall. A part of

I_{total} , being the plasma sheath current I_p , lifts off the back-wall insulator and drives a shock wave axially down the coaxial space. At the end of the anode, the plasma sheath turns from axial into radial motion. The previously axially moving I_p becomes a radial inward moving cylindrical sheath, driving a radially collapsing cylindrical shock front. When this shock front arrives on axis, because the plasma is collisional, a reflected shock (RS) moves radially outwards¹¹ until it meets the incoming driving current sheath. The increased pressure of the RS region then rapidly slows down the sheath. This is the start of the pinch phase. All the dynamics dominating the axial and radial phases is determined by I_p . A proportion of the current, the difference between I_{total} and I_p , does not take part in the dynamics. This leakage current stays at the back wall,^{4–7,12} but parts of it may be diffusely distributed.

We define for the axial phase f_c as I_p/I_{total} and distinguish it from f_{cr} for the radial phase. Likewise, it had been shown that only a fraction of the mass^{6,12} encountered by the axial sheath is swept up. This fraction we call f_m , distinguishing the radial phase fraction as f_{mr} . The rest of the mass either leaks through the sheath or is swept outwards due to the canting of the sheath.

The exact time profile of the I_{total} trace is governed by the bank, tube, the operational parameters, and by the mass and current fractions and variation of these fractions through the axial and radial phases. Although we may expect these fractions to vary, for simplicity, we average these model parameters as f_m , f_c and f_{mr} and f_{cr} .

The Lee model couples the electrical circuit with plasma focus dynamics, thermodynamics, and radiations enabling realistic simulation of all gross focus properties. The basic model was described in 1984 (Ref. 13) and used to assist projects.^{6,7,10,11,14–16} An improved five-phase code crucially incorporating small disturbance speed,¹⁷ and radiation coupling with dynamics, assisted further projects,^{8,18–23} and was published in the internet in 2000 (Ref. 24) and 2005.²⁵ Plasma self-absorption was included²⁴ in 2007. It has been used in machines including UNU/ICTP PFF,^{10,11,15,16,21} NX2,^{18–20} and NX1,¹⁸ and has been adapted to the Filippov-type DENA.^{8,22,23} Neutron yield Y_n using a beam-target mechanism,¹ is included in the present version RADPFV5.13, (Ref. 26) resulting in realistic Y_n scaling²⁷ with I_{pinch} . Since

^{a)}Electronic mail: leesing@optusnet.com.au.

the detailed theory of the model and the code are given in the websites,^{24–26} we proceed to the proposed method to compute I_{pinch} .

The method requires a measured I_{total} waveform from a discharge in which the bank parameters, the tube geometry, and operating parameters are known. The Lee model code²⁶ is used to simulate this discharge using the model parameters for fitting. The model parameters are varied until the simulated I_{total} trace agrees with the measured I_{total} trace. The start of the quiescent or pinch phase is pinpointed from the computation and the computed value of I_p at this time is obtained as I_{pinch} .

For the actual fitting process, the bank parameters L_0 , C_0 (capacitance), and r_0 (resistance) are put into the active sheet of the EXCEL code. If r_0 is not available, a trial value of $0.1(L_0/C_0)^{1/2}$ is used. Next, the tube parameters b (cathode radius), a (anode radius), and z_0 (anode length) and the operational parameters V_0 (voltage) and P_0 (pressure) are entered. The fill gas is indicated by its atomic weight and number in the cells provided. Trials values of f_m , f_c , f_{mr} , and f_{cr} are then entered, e.g., 0.08, 0.7, 0.1, and 0.7, respectively. The code is then run. The computed I_{total} trace which is one of the graphical outputs is transferred onto a comparison active sheet and plotted onto a graph together with the pre-loaded measured I_{total} trace. Detailed comparison, feature by feature, of the traces is made.

The first step is fitting the axial phase. This involves variation of f_m and f_c while observing the changes that appear on the resulting computed I_{total} trace in respect to the rise time, rising shape, and I_{peak} and how these features compare with the corresponding features of the measured I_{total} trace. During this fitting an increase in f_c increases axial speed which increases dynamic resistance, thus, lowering current magnitude on the rising slope. The greater rate of increase of tube inductance flattens out the rising slope. A decrease in f_m has almost the same effect. However, a change in f_c has an additional subtle effect of changing the relative effect of the tube inductance. This means that increasing the speed by a certain amount by increasing f_c , then reducing it by exactly the same amount by a corresponding increase in f_m will not bring the I_{total} shape and magnitude back to the shape and value before either change is made. Thus, one has to get each of f_m and f_c separately correct to get both the current shape and magnitude correct in the rising current profile.

The value of r_0 may need to be adjusted. An increase of r_0 lowers the current trace at all points proportionately. Adjustment to nominally given values of L_0 , sometimes even C_0 , may need to be made before a good fit is achieved. When all values are properly adjusted and when f_m and f_c are correctly fitted, the measured rising profile of the computed I_{total} , usually up to the peak value I_{peak} , is found to fit the measured rising profile well in both shape and magnitude.

Two other points need to be noted.^{6,7} The measured I_{total} profile usually has a starting portion which seems to rise more slowly than the computed trace. This is due to the switching process during which, until fully switched, the spark gap presents additional resistance. It could also be compounded by the lift-off delay.²¹ Practically, this effect is compensated by shifting the whole computed trace forward in time, usually by a small amount around 50 ns. A related note is that z_0 may need to be reduced to account for the shape of the back-wall insulator.

Author complimentary copy. Redistribution subject to AIP license or copyright, see <http://apl.aip.org/apl/copyright.jsp>

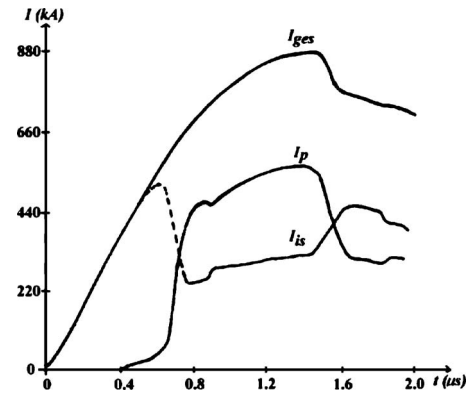


FIG. 1. DPF78 measured I_{total} (labeled as I_{ges}) and measured I_p waveforms. The third trace I_{is} is the difference of I_{total} and I_p .

The next step is fitting the radial phases. We need to understand the transition from the axial to the radial phase. For a plasma focus to work well, it is usually operated with a speed such that its axial run-down time is about equal to the rise time of the circuit with the device short circuited across its back wall. With the focus tube connected, the current rise time will be larger. At the same time, the current trace is flattened out. In most cases this increased rise time will be cut short by the start of the radial phase. As this phase starts, the current trace starts to roll over, at first imperceptibly, then clearly dipping and then sharply dips as the focus dynamics enters the severe pinch phase which absorbs a significant portion of the energy from the driving magnetic field. Thus, the second step in the fitting consists of adjusting f_{mr} and f_{cr} so that the computed current roll over and the dip agree in shape, slope, and extent of dip with the measured waveform.

We now describe how we tested the validity of this method. In an experiment in Stuttgart using the DPF78,^{4,5} a Rogowski coil measured the I_{total} trace, and magnetic probes measured the I_p waveform. The bank parameters were $C_0 = 15.6 \mu\text{F}$ (nominal) and $L_0 = 45 \text{ nH}$ (nominal), tube parameters were $b = 50 \text{ mm}$, $a = 25 \text{ mm}$, and $z_0 = 150 \text{ mm}$, and operating parameters were $V_0 = 60 \text{ kV}$, and $P_0 = 7.6 \text{ Torr}$ deuterium. Figure 1 shows these measured I_{total} (labeled as I_{ges} in Fig. 1) and I_p waveforms. The third trace is the difference of I_{total} and I_p .

These parameters were put into the code. The best fit for the computed I_{total} with the measured I_{total} waveform was obtained with the following: bank parameters were $C_0 = 17.2 \mu\text{F}$, $L_0 = 55 \text{ nH}$, and $r_0 = 3.5 \text{ m}\Omega$; tube parameters were $b = 50 \text{ mm}$, $a = 25 \text{ mm}$, and $z_0 = 137 \text{ mm}$; and operating parameters were $V_0 = 60 \text{ kV}$ and $P_0 = 7.6 \text{ Torr}$ deuterium. Model parameters of $f_m = 0.06$, $f_c = 0.57$, $f_{mr} = 0.08$, and $f_{cr} = 0.51$ were fitted.

With these parameters, the computed I_{total} trace compared well with the measured I_{total} trace, as shown in Fig. 2. The computed dynamics, currents, and other properties of this plasma focus discharge were deemed to be correctly simulated.

From the computation results the start of the pinch phase was obtained as $1.551 \mu\text{s}$. At this time I_{pinch} was computed as $0.51 \times 778 = 396.8 \text{ kA}$. The value of I_{pinch} from the measured I_p trace was not immediately obvious since there was no striking feature that marked this moment on the measured I_p trace. We used the following procedure to obtain it, at the

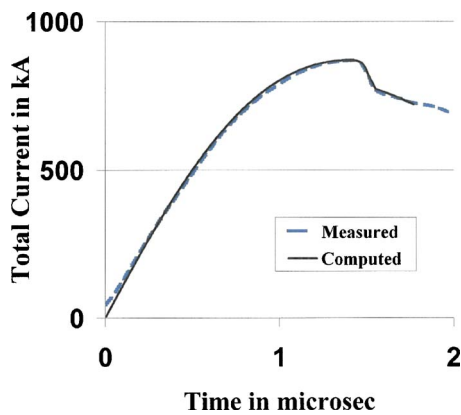


FIG. 2. (Color online) Comparison of computed (solid line) and measured (dashed line) I_{total} waveforms.

same time to get further insight into f_c and f_{cr} .

The ratio I_p/I_{total} (digitized from Fig. 1) was plotted as a function of time and shown in Fig. 3. At time = 1.551 μs , the ratio was found to be 0.49, and I_{total} was measured to be 778 kA. Hence, $I_{\text{pinch}} = 381.2$ kA was measured in the Stuttgart DP78 experiment. The computed I_{pinch} was 4% larger than the measured I_{pinch} . This difference was to be expected considering that the modeled f_{cr} was an average value of 0.51; while the laboratory measurement showed (Fig. 3) that in the radial phase I_p/I_{total} varied from 0.63 to 0.4, and at the start of the pinch phase this ratio was 0.49 and rapidly dropping. Thus, one would expect the computed value of I_{pinch} to be somewhat higher than the measured, which turned out to be the case. Nevertheless, the difference of 4% is better than the typical error of 20% estimated for I_{pinch} measurements using magnetic probes.³

The conclusion is that the numerical method is a good alternative, being more accurate and convenient and only needing a commonly measured I_{total} waveform.

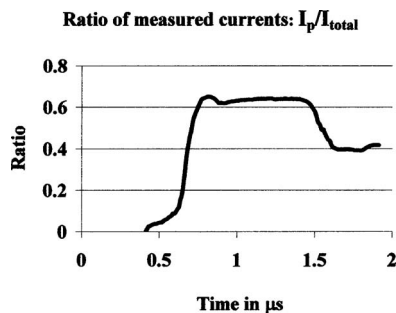


FIG. 3. Ratio of measured I_p to I_{total} as a function of time.

- ¹V. A. Gribkov, A. Banaszak, B. Bienkowska, A. V. Dubrovsky, I. Ivanova-Stanik, L. Jakubowski, L. Karpinski, R. A. Miklaszewski, M. Paduch, M. J. Sadowski, M. Scholz, A. Szydlowski, and K. Tomaszewski, *J. Phys. D* **40**, 3592 (2007).
- ²L. Soto, P. Silva, J. Moreno, G. Silvester, M. Zambra, C. Pavez, L. Altamirano, H. Bruzzone, M. Barbaglia, Y. Sidelnikov, and W. Kies, *Braz. J. Phys.* **34**, 1814 (2004).
- ³H. Herold, in *Laser and Plasma Technology*, Proceedings of Third Tropical College, edited by C. S. Wong, S. Lee, B. C. Tan, A. C. Chew, K. S. Low, and S. P. Moo (World Scientific, Singapore, 1990), pp. 21–45.
- ⁴T. Oppenländer, Ph.D. thesis, University of Stuttgart, Germany, 1981.
- ⁵G. Decker, L. Flemming, H. J. Kaeppler, T. Oppenlander, G. Pross, P. Schilling, H. Schmidt, M. Shakhatre, and M. Trunk, *Plasma Phys.* **22**, 245 (1980).
- ⁶T. Y. Tou, “Pinch radius ratio of the plasma focus,” Ph.D. Thesis, University of Malaya, 1986.
- ⁷T. Y. Tou, S. Lee, and K. H. Kwek, *IEEE Trans. Plasma Sci.* **17**, 311 (1989).
- ⁸V. Siahpoush, S. Sobhanian, S. Khorram, and M. A. Tafreshi, ICOPS 2003, IEEE Conference Record, 2003 (unpublished), 444.
- ⁹S. Lee and S. H. Saw, *Appl. Phys. Lett.* **92**, 021503 (2008).
- ¹⁰S. Lee, T. Y. Tou, S. P. Moo, M. A. Elissa, A. V. Gholap, K. H. Kwek, S. Mulyodrono, A. J. Smith, S. Suryadi, W. Usala, and M. Zakaullah, *Am. J. Phys.* **56**, 62 (1988).
- ¹¹S. Lee and A. Serban, *IEEE Trans. Plasma Sci.* **24**, 1101 (1996).
- ¹²S. P. Chow, S. Lee, and B. C. Tan, *J. Plasma Phys.* **8**, 21 (1972).
- ¹³S. Lee, in *Radiations in Plasmas*, edited by B. McNamara (World Scientific, Singapore, 1984), pp. 978–987.
- ¹⁴S. Lee, *IEEE Trans. Plasma Sci.* **19**, 912 (1991).
- ¹⁵M. H. Liu, X. P. Feng, S. V. Springham, and S. Lee, *IEEE Trans. Plasma Sci.* **26**, 135 (1998).
- ¹⁶S. Lee, “Twelve years of UNU/ICTP PFF—A review,” ICTP OAA report, 1998 (unpublished).
- ¹⁷D. E. Potter, *Phys. Fluids* **14**, 1911 (1971).
- ¹⁸S. Lee, P. Lee, G. Zhang, X. Feng, V. A. Gribkov, M. Liu, A. Serban, and T. Wong, *IEEE Trans. Plasma Sci.* **26**, 1119 (1998).
- ¹⁹S. Bing, “Plasma dynamics and x-ray emission of the plasma focus,” Ph.D. thesis, Nanyang Technological University, Singapore, 2000.
- ²⁰D. Wong, P. Lee, T. Zhang, A. Patran, T. L. Tan, R. S. Rawat, and S. Lee, *Plasma Sources Sci. Technol.* **16**, 116 (2007).
- ²¹T. Zhang, X. Lin, K. A. Chandra, T. L. Tan, S. V. Springham, A. Patran, P. Lee, S. Lee, and R. S. Rawat, *Plasma Sources Sci. Technol.* **14**, 368 (2005).
- ²²V. Siahpoush, M. A. Tafreshi, S. Sobhanian, and S. Khorram, *Comments Plasma Phys. Controlled Fusion* **47**, 1065 (2005).
- ²³S. Goudarzi, R. Amrollahi, and R. Saberi Moghaddam, *J. Fusion Energy* (to be published).
- ²⁴S. Lee, Radiative Dense Plasma Focus Computation Package RADPF, (<http://ckplee.myplace.nie.edu.sg/plasmaphysics/>).
- ²⁵S. Lee, in ICTP Open Access Archive, 2005 (<http://eprints.ictp.it/85/>).
- ²⁶S. Lee, Radiative Dense Plasma Focus Computation Package RADPF, (<http://www.intimal.edu.my/school/fas/UFLF/>).
- ²⁷S. Lee and S. H. Saw, *J. Fusion Energy* (to be published).